



HHS Public Access

Author manuscript

Int J Pharm. Author manuscript; available in PMC 2018 August 30.

Published in final edited form as:

Int J Pharm. 2017 August 30; 529(1-2): 32–43. doi:10.1016/j.ijpharm.2017.06.042.

Ocular Disposition of Ciprofloxacin from Topical, PEGylated Nanostructured Lipid Carriers: Effect of Molecular Weight and Density of Poly (ethylene) glycol

Sai Prachetan Balguri¹, Goutham R Adelli¹, Karthik Yadav Janga¹, Prakash Bhagav¹, and Soumyajit Majumdar^{1,2}

¹Department of Pharmaceutics and Drug Delivery, School of Pharmacy, The University of Mississippi, University, MS 38677

²Research Institute of Pharmaceutical Sciences, School of Pharmacy, The University of Mississippi, University, MS 38677

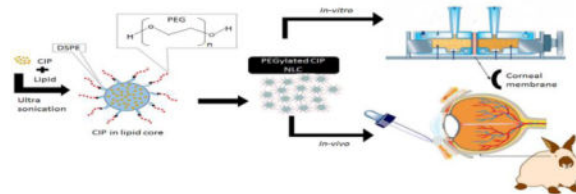
Abstract

Ciprofloxacin (CIP) is an antibacterial agent prescribed for the treatment of ocular infections. The objective of the present project is to investigate the effect of surface PEG functionalization of the Nano structured lipid carriers (NLCs) on formulation stability, ocular penetration and distribution. CIP NLCs were tested with different molecular weight (poly ethylene glycol) PEGs ranging from (2K to 20K) grafted onto the phospholipid and with different chain lengths (14–18 carbons) of phospholipids derivatized with PEG-2K. Drug load in the formulations was maintained at 0.3% w/v. Formulations prepared were evaluated with respect to *in vitro* release, transcorneal permeation, autoclavability, morphological characteristics and *in vivo* ocular tissue distribution. Scanning Transmission electron microscopy (STEM) studies revealed that the PEG-CIP-NLCs were spherical in shape. Transcorneal penetration of CIP was optimum with PEG molecular weight in between 2K to 10K. Carbon chain length of the phospholipid, however, did not affect transcorneal penetration of CIP. *In vivo* ocular tissue CIP concentrations attained from the various formulations was consistent with the *in vitro* data obtained. The results suggest that surface functionalization of PEGs, within a specified range of molecular weight and surface packing density, significantly enhance trans-ocular penetration and impart sterilization-stabilization characteristics into the formulations.

Graphical abstract

Sai Prachetan Balguri, sbalguri@go.olemiss.edu, 361-522-7682
Goutham R Adelli, gradelli89@gmail.com, 662-202-6204
Karthik Yadav Janga, kjanga@go.olemiss.edu, 662-915-7641
Prakash Bhagav, prakashbhagav@gmail.com, 662-638-5207
Soumyajit Majumdar, majumso@olemiss.edu, 662-915-3793

Publisher's Disclaimer: This is a PDF file of an unedited manuscript that has been accepted for publication. As a service to our customers we are providing this early version of the manuscript. The manuscript will undergo copyediting, typesetting, and review of the resulting proof before it is published in its final citable form. Please note that during the production process errors may be discovered which could affect the content, and all legal disclaimers that apply to the journal pertain.



Keywords

Ciprofloxacin; Surface functionalized NLCs; PEGylation; Chitosan chloride; PEG derivatized phospholipids; transcorneal penetration; topical lipid nanoparticles

1. Introduction

Delivery of drugs, especially to the back-of-the eye tissues comprising sclera, choroid, retina, and vitreous body, is restricted by multiple physiological processes, anatomic, static, dynamic and efflux barrier functionalities (1, 2). Efflux protein pumps expressed on ocular tissues restrict transmembrane permeability of drugs, thus lowering penetration of substrates from the systemic, topical or periocular routes (3, 4). Topical application is the most favored route because of the ease of administration, lack of associated complications and minimal nonspecific systemic exposure. Only 5–10% of the topically administered dose, however, reaches the inner ocular tissues (5, 6). Although advances have been made with respect to delivery into the anterior segment ocular tissues, significant challenges still exist for very lipophilic molecules in view of the formulation restrictions placed by the sensitivity of the ocular tissues. Several formulation approaches such as inclusion of viscosity enhancers in aqueous ophthalmic solution or suspension formulations, ion-exchange resin based formulations, implants, transporter targeted systems, emulsions, films and other nanoparticle mediated drug delivery strategies have been described in the literature, and some are commercially available (7–10). Despite technological advancements in the formulation strategies, delivery of therapeutic agents efficiently into the back-of-the eye ocular tissues through the topical route remains elusive (11). Ointments have been successful to some extent but various drawbacks, including difficulty in application and problems in vision, have limited its usefulness. Success in back-of-the eye delivery mainly depends on formulation platform, candidate's physicochemical properties and absorption pathway. Penetration of drugs across alternatively polarized (lipophilic and hydrophilic) ocular layers, and through the corneal tight junctions, is highly dependent upon their physicochemical properties. Thus, the molecules should exhibit optimum physicochemical aspects and are to be formulated in appropriate dosage forms for enhanced retinal delivery (12, 13).

Kinetics, bio-distribution and release profile of drugs could be dramatically modulated with nano particulate systems (14, 15). Nanoparticles have been observed to exhibit superior penetration characteristics into the inner ocular tissues compared to solution or suspension formulations (16). Lipid based systems such as nanostructured lipid carriers (NLCs) are potential carriers for therapeutic agents, especially hydrophobic molecules, and possess favorable properties including but not limited to biocompatibility, mucoadhesion, penetration /retention capability, lower clearance rate, controlled release, greater stability

and protection of the drug candidate from chemical degradation. NLC's can be formulated from a wide variety of lipids (solid/liquid) and phospholipid combinations with varying composition, to achieve desired morphometrical, physicochemical, surface charge and release characteristics. Mixture of solid and liquid lipids used in NLC's create imperfections in the crystal lattice accommodating higher drug loads while maintaining similar penetration capabilities as the solid lipid nanoparticulates (SLNs). In addition, NLCs allow higher drug loading compared to SLNs, exhibit better encapsulation efficiency, lesser drug expulsion and higher stability (17–19). Reports suggest that PEGylated amphiphilic lipids possess the ability to transform into lipid based lyotropic crystals with thermodynamically stable self-assembled structures in aqueous environment (20, 21). In recent years, PEGylation technology (functionalization of nano carriers with PEG's and appropriate ligands) has been widely used to improve the pharmacokinetics, bioavailability and tissue distribution characteristics of a variety of nanoparticles, because the hydrophilic and inert PEG creates a steric barrier on the surface of nanoparticles and minimizes protein binding (22). The bulky and highly hydrated corona of the PEG extending from the lipid bilayer into the aqueous phase is critical for enhancing steric stabilization of the nanoparticles (23). Also, incorporation of PEG could allow better stabilization against aggregation, on storage and on sterilization - by amorphization and inducing imperfections in crystal lipid lattices (24, 25).

Ciprofloxacin (CIP) belongs to class of fluoroquinolone antibiotics and is active against a broad spectrum of gram-positive and gram-negative bacteria. It is usually prescribed as the first line of treatment for corneal keratitis, allergic conjunctivitis and other bacterial infections of the eye. CIP is a zwitterion with pKa values of 6.0 (acidic group) and 8.8 (basic group) and an isoelectric point of 7.2 where it is least soluble (neutral species). The compound is currently marketed as an ophthalmic solution and needs frequent dosing due to its poor ocular bioavailability (26). Because of solubility issues, the formulation has to be maintained at an acidic pH. On topical application, however, because of the buffering action of the tear fluid, the pH of the instilled formulation is quickly neutralized as a result of which the solubility of CIP in that environment is significantly reduced and precipitation can take place. Consequently, penetration of CIP into the interior ocular tissues is hampered. In general, there exists a need to enhance drug penetration into the ocular tissues through the topical route. Moreover, improved delivery and penetration of ocular drugs with solubility issues, such as CIP, would be highly beneficial for intervening in complications associated with bacterial infections.

The objective of the current research is to assess the effect of type and density of surface PEGylation of CIP loaded NLCs in terms of process (including autoclave sterilization) and storage stability characteristics and ocular disposition.

2. Materials and Methods

CIP was obtained from Sigma Aldrich (St. Louis, MO). DSPE-mPEG-1000, DSPE-mPEG-10000, DSPE-mPEG-20000, (N-Carbonyl-methoxypolyethylene glycol-5000)-1,2 di-myristoyl-sn-glycero phosphoethanolamine (DMPE-mPEG-5000) were received from Creative PEG Works (Winston Salem, NC). 1,2-dipalmitoyl-sn-glycero phosphoethanolamine (DPPE), DMPE-mPEG-2000, and DPPE-mPEG-2000 were obtained

from NOF America Corporation (White Plains, NY). DSPE-sodium (C₁₈), DMPE-sodium (C₁₄), DPPE-sodium (C₁₆), DSPE-mPEG-2000 and DSPE-PEG-5000 were obtained from Lipoid® (Ludwigshafen Germany). Glycerol Monostearate was obtained as a gift sample from Gattefossé (Paramus, NJ). Amicon® Ultra centrifugal filter devices with regenerated cellulose membrane (molecular weight cut off 100 kDa), Poloxamer 188, Tween®80, high performance liquid chromatography (HPLC) - grade solvents, and other chemicals (analytical grade) were obtained from Fisher Scientific (Hampton, NH). Whole eyes of male albino New Zealand rabbits were obtained from Pel-Freez Biologicals (Rogers, AR). Male albino New Zealand rabbits were procured from Harlan Labs (Indianapolis, IN).

2.1. Formulations

CIP-NLCs and PEGylated CIP-NLCs (PEG-CIP-NLCs)—Glycerol monostearate (GMS), DSPE-sodium C₁₈ (phospholipid) and oleic acid (liquid lipid) were used to prepare the DSPE-CIP-NLCs by ultra-sonication method. Briefly, GMS and oleic acid were melted, DSPE-sodium salt was added in small increments to form homogenous lipid mixture and then CIP was dispersed therein to obtain a lipid phase. An aqueous phase, containing surfactants (Poloxamer 188 (0.25% w/v) and Tween® 80 (0.75% w/v) and glycerin (2.25% w/v) in bi-distilled water, was heated. The hot aqueous phase was then added to the melted lipid phase under stirring to form a premix. The premix was then sonicated at 16,000 rpm for 6 min using T 25 digital Ultra-Turrax to form a hot pre-emulsion. The pre-emulsion obtained, was subjected to ultra-sonication (Vibracell™) at an amplitude of 80 for 6 min resulting in the formation of hot emulsion dispersion. The hot emulsion obtained was slowly cooled to room temperature to form NLCs. The pH of the resulting formulation was adjusted to 5.0 using 0.1 N NaOH.

A portion of the phospholipids in the DSPE-CIP-NLC formulations were replaced with PEGylated phospholipids, N-(Carbonyl-methoxypolyethylene glycol-2000)-DSPE (DSPE-mPEG2000), to prepare the PEG-CIP-NLCs (PEG(2K)-CIP-NLC). Total amount of the lipid in the NLCs was 6% of which solid lipid constituted 50% and oleic acid made up the remaining 50%. Drug load in the formulations was maintained at 0.3% w/v.

Additional PEG-CIP-NLCs were prepared wherein the molecular weight of the PEG (1K, 2K, 5K, 10K and 20K) grafted to DSPE was varied (DSPE-mPEG-1K/DSPE-mPEG-5K / DSPE-mPEG-10K/DSPE-mPEG-20K) to study the effect of the PEG molecular weight on the biopharmaceutical characteristics of the NLCs. CIP formulations were also prepared with mPEG-2K derivatized phospholipids of different chain lengths such as PEG 2000-1,2-dimyristoyl/dipalmitoyl-sn-glycero-3-phosphoethanolamine, sodium salt (DMPE C₁₄/DPPE C₁₆). These formulations, wherein the PEG molecular weight is constant (2K) but the lipid chain length is different (DPPE and DMPE), were designed to understand the role of the phospholipid chain-length on the PEG-CIP-NLC characteristics. A detailed description of the composition of all the CIP-NLC and PEG-CIP-NLC formulations tested, including the associated formulation codes used, have been presented in Table 1. All the components (lipids/surfactants) used in the formulations are represented by weight (mg).

Table 5 includes several placebo formulations (SLNs/NLCs) prepared using different lipid (solid/liquid) mixtures (combinations varying composition and/or total lipid content) tested

for physical autoclave stability. The lipid excipients and surfactants used in the formulation are represented by weight (mg). Two batches (n=2) of formulations each with batch size of 10.6 g (volume ~10 mL) were used for stability testing. NLCs that were unstable on autoclaving were reformulated by replacing 50% of the phospholipid (DSPE) with PEGylated (2K) DSPE to yield PEG(2K)-NLCs. The effect of PEG surface packing density (0–40%) and molecular weight (1K, 2K and 5K) on the autoclave stability of the PEG-NLCs was subsequently studied.

Chitosan coated NLCs (CIP-ChCl-NLCs) and CIP control solution—The DSPE-CIP-NLC formulation was coated with chitosan chloride (ChCl – 0.25% w/v) by adding ChCl solution into the final formulation (Table 1). Surface adsorption was confirmed by way of change in the zeta potential value.

CIP control formulation—Marketed CIP ophthalmic Solution 0.3% w/v was used as control formulation for the studies (Mfg. By: Hi-Tech Pharmacal; Lot # 622553).

2.2. Particle size, zeta potential and polydispersity Index (PDI) measurement

The hydrodynamic radius and the PDI of the NLC formulations were determined by photon correlation spectroscopy, using Zetasizer Nano ZS Zen3600 (Malvern Instruments, Inc.) at 25°C and 173° backscatter detection, in disposable clear cells. The measurements were obtained using a helium-neon laser of 633 nm, and the particle size analysis data was evaluated using volume distribution. Zeta potential measurements were carried out at 25°C in disposable cells using the same instrument. For measurement of particle size distribution and zeta potential, NLC samples were diluted (1:500) with water. Bi-distilled and 0.2 µM filtered water was used for these measurements, and were performed in triplicates.

2.3. Scanning transmission electron microscopy (STEM) studies

Lipid nanoparticulate formulations were characterized by scanning transmission electron microscope (Zeiss Auriga®-40 dual beam) using 1% w/v uranyl acetate as a stain. A freshly glow discharged 200 mesh copper grid with a thin carbon was used as a base support for the sample. A small drop (10–20 µL) of sample was placed on a piece of parafilm and the grid was floated on top of the sample for 30 sec, then the grid was removed and excess sample was blotted using a piece of filter paper. Grid was then floated on a drop of distilled water for 10 sec, the water was removed and the grid with sample was floated on a drop of stain for 1 min after which excess stain was blotted again. After drying for at least 30 min, the samples were imaged in a Zeiss Libra operating at 30kV and in STEM mode.

2.4. Analytical method for *in vitro* sample analysis

Samples were analyzed for CIP content using an HPLC-UV method. The system comprised of Waters 717 plus Autosampler, Waters 2487 Dual λ Absorbance detector, Water 600 controller pump, and Agilent 3395 Integrator. A Phenomenex Luna® C₁₈ 4.6 mm × 250 mm column was used under isocratic elution for chromatographic analysis. The mobile phase used was mixture of acetonitrile and triethanolamine buffer (150:850 v/v) with pH adjusted to 2.36 using orthophosphoric acid. Triethanolamine buffer is made up of water,

triethanolamine and 25 mM phosphoric acid in the ratio of (996:1.6:1.57 v/v). The flow rate was set at 1 mL/min with λ_{\max} (detection wavelength) of 299 nm during the analysis (27).

2.5. Assay and Entrapment Efficiency

The assay (total drug content) is determined in the CIP NLC formulations. The lipid in the DSPE-CIP-NLC and PEG-CIP-NLC formulations was precipitated using 50:50 binary mixture of 0.1N HCl and 190-proof alcohol and, drug content in the supernatant after centrifugation (13,000 rpm for 20 min), was measured using an HPLC system following appropriate dilution. The percentage of CIP entrapped (% EE) in DSPE-CIP-NLC and PEG-CIP-NLC was determined by measuring the concentration of free drug in the aqueous phase of an undiluted formulation. The EE was evaluated by an ultrafiltration technique with a 100 kDa centrifugal filter device (Amicon Ultra). An aliquot (500 μ L) of the corresponding formulation was added to the sample reservoir and centrifuged at 5,000 rpm for 10 min. The filtrate was analyzed for drug content using HPLC. The %EE was calculated using Eq. (1) below. All the measurements were carried out in triplicates.

$$\%EE = \left[\frac{w_i - w_f}{w_i} \right] \times 100 \quad (1)$$

Where W_i =total drug content, and W_f =amount of free drug in aqueous phase.

2.6. Terminal moist heat sterilization and stability assessment of CIP formulations

CIP loaded NLCs (DSPE-CIP-NLC and PEG-CIP-NLCs) and placebo formulations were prepared and put into appropriately labelled glass vials, affixed with sterilization indicator tapes, subjected to moist-heat sterilization (121°C for 15 min under 15 psi), in thermo-controlled autoclave (AMSCO® Scientific Model SI-120). Stabilizing agents and cloud point modifiers such as polyvinyl pyrrolidone (PVP K30), polyvinyl alcohol (PVA Avg Mol wt 30K–70K Da), PEG 400, PEG 1000, PEG 4000, PEG 6000 at concentrations of 0.25% and 0.5% w/v were used in the DSPE-CIP-NLCs. Following autoclaving, sterilized samples were evaluated in terms of physical appearance, color, morphometrical and physicochemical characteristics against unsterilized reference formulations kept at room temperature. Sterilization cycle was confirmed by change in the color of indicator tapes on the glass vials.

2.7. *In vitro* release studies

In vitro release of CIP from the respective formulations such as marketed CIP ophthalmic control solution (0.3% w/v), DSPE-CIP-NLCs and PEG (2K)-CIP-NLCs were evaluated using Valia-Chien® cells (PermeGear, Inc.). Spectra/por® membrane (3.5K MWCO) was mounted on diffusion cells between donor/receptor chambers and fastened with clamps, through which transport kinetics were studied. The temperature of the cells was maintained at 34°C with the help of a circulating water bath. Five milliliters of isotonic phosphate buffer (IPBS - pH 7.4) containing 2.5% w/v RM β CD was used as the receptor media during the course of the experiment (6 h). Five hundred microliters of the formulations was added into the donor chamber. Aliquots (600 μ L) were withdrawn from the receiver chamber and replaced with an equal volume of the 2.5% w/v RM β CD in IPBS (pH 7.4) solution at

predetermined time points. Donor CIP concentration was maintained at 0.3% w/v in all the formulations. Samples taken were analyzed using high performance liquid chromatography-UV (HPLC-UV) system.

2.8. *In vitro* corneal permeation studies

The corneas excised from whole eyes, obtained from Pel-Freez Biologicals, were used for the determination of *in vitro* transcorneal permeability. Whole eyes were shipped overnight in Hanks balanced salt solution, over wet ice, and were used immediately upon receipt. The corneas were excised with some scleral portion to help secure the membrane onto the diffusion cells. After excision, the corneas were washed with the (IPBS; pH 7.4) and mounted on Valia-Chien cells (PermeGear, Inc[®]) with the epithelial side facing the donor chamber. The temperature of the cells was maintained at 34°C with the help of a circulating water bath. Five hundred microliters of CIP formulations (CIP ophthalmic control solution, DSPE-CIP-NLCs and PEG (2K)-CIP NLCs) was added to the donor chamber and the CIP concentration was maintained at 0.3% w/v in formulations. The receiver chamber consisted of 5 mL of RM β CD (2.5% w/v) in IPBS (pH 7.4) solution for all the transport studies. Aliquots (600 μ L) were withdrawn from the receiver chamber at predetermined time points, until 3 h, and replaced with an equal volume of receiver medium. Samples were stored at -80°C until further analysis.

Additionally, effect of carbon chain length (DMPE/DPPE/DSPE-mPEG-2000) and molecular weight of PEG's (DSPE-PEG-1K/2K/5K) on transcorneal permeability of CIP from PEG-CIP-NLCs was investigated using side-by-side diffusion apparatus. Three milliliter's of CIP formulations was added to the donor chamber and receiver medium consisted of 3.2 mL of RM β CD (2.5% w/v) in the IPBS (pH 7.4). A slight difference in the donor and receiver chamber volumes helped to maintain the normal corneal curvature through marginally elevated hydrostatic pressure. The contents of both chambers were stirred continuously with a magnetic stirrer. Aliquots (600 μ L) were withdrawn from the receiver chamber at predetermined time points until 3 h and replaced with an equal volume of the solution.

2.9. Biosample preparation for determination of CIP in ocular tissue homogenates

In vivo sample analysis was carried out using a previously validated HPLC-UV method following method revalidation. Mixture of ice cold acetonitrile and 0.1% formic acid (1 mL) was added to the sample to precipitate proteins and extract the drug from individual, tissues namely cornea, sclera, iris-ciliary (IC) and retina-choroid (RC), after cutting them into small pieces. The samples were centrifuged for 1 h at 13,000 rpm and the supernatant was then collected for further analysis. Aqueous humor (AH) (200 μ L), vitreous humor (VH) (500 μ L) tissues were precipitated by adding an ice cold mixture of acetonitrile & formic acid; 200 μ L for AH and 500 μ L for VH in the ratio (1:1). Standard calibration curves constructed from various ocular tissues such as cornea (20–500 ng/mL), sclera (20–500 ng/mL), AH (10–200 ng/mL), VH (10–200 ng/mL), IC (10–200 ng/mL), RC (10–200 ng/mL) were used to determine the drug concentration in the samples. All the standard curves had a coefficient of determination $r^2 = 0.96$. The accuracy and precision of the bio-analytical method was determined by analyzing the quality control (QC) drug samples of all ocular matrices at

three different concentration levels (50,100,200 ng/mL) each prepared in sextuplicate ($n=6$). The inter-day and intra-day variabilities in precision (% RSD) ranged between 3.97–12.6% and 4.57–9.78% in ocular tissue homogenates tested. The intra-assay and inter-assay accuracies, expressed as the percentage difference between the measured concentration and the nominal concentration ranged from –7.57% to 11.35% and –10.3% to 12.6% in ocular tissues respectively. The precision and accuracies of the QC samples obtained met the requirements set forth under bioanalytical guidance (Guidance for Industry: bioanalytical method validation in Food and Drug Administration guidelines of September 2013) (28). Recovery of CIP was evaluated by spiking drug in blank tissues and comparing the expected CIP concentration with standard concentration. Recovery values were observed in AH (90.3%), VH (92.9%), cornea (89.7%), sclera (87.2%), IC (91.5%) and RC (93.3%). Interference was not observed from co-eluted protein residues with respect to CIP peaks in all the tissues. Limit of Detection (LOD) in various ocular tissues was determined in AH (10 ng/mL), VH (10 ng/mL), cornea (20 ng/mL), sclera (20 ng/mL), RC and IC (10 ng/mL).

2.10. *In vivo* bioavailability studies

In vivo bioavailability of CIP was determined in conscious Male New Zealand albino rabbits weighing between (2–2.5 kg), procured from Harlan labs. All the animal studies conformed to University of Mississippi Institutional Animal Care and Use Committee (IACUC) and Association for research in vision and ophthalmology (ARVO) approved protocols. CIP formulations namely marketed ophthalmic control solution, DSPE-CIP-NLCs and PEG (1K/2K/5K/20K)-CIP-NLCs were evaluated *in vivo*. These topical formulations (100 μ L) were instilled as two doses (50 μ L each dose) at two different time points, –30min and 0 min, to reduce pre-corneal loss. At the end of 2 h post application of the second drop (0 min), rabbits were euthanized with an overdose of pentobarbital, injected through a marginal ear vein. The eyes were washed thoroughly with ice cold DPBS and were immediately enucleated. The intraocular tissues were separated and stored at –80 °C until further analysis using an HPLC-UV system. All experiments were carried out in triplicate.

2.11. Data analysis

The steady-state flux (SSF) for transcorneal experiments was calculated by dividing the rate of transport by the surface area. Flux was calculated using Eq. (2).

$$\text{Flux}(J)=(dM/dt)/A \quad (2)$$

Where, M is the cumulative amount of drug transported, and A is the surface area of the corneal membrane (0.636cm²) exposed to the permeant (drug).

The transcorneal permeability was determined by normalizing the SSF to the donor concentration, C_d , according to Eq. (3).

$$\text{Permeability}(P_{app})=\text{Flux}/C_d \quad (3)$$

2.12. Statistical analysis

One way-ANOVA coupled Post-Hoc test was employed to analyze the differences between groups. Data obtained was considered to be statistically significant at level of ($p < 0.05$).

3. Results

3.1. Physicochemical characteristics of CIP containing lipid nanoparticle formulations

A detailed description of the composition of all the CIP-NLC and PEG-CIP-NLC formulations tested, including the associated formulation codes used, have been presented in Table 1. Physicochemical characteristics of the various NLCs are presented in Table 2. Hydrodynamic radii of all the NLC formulations did not vary significantly whereas the entrapment efficiency values with the PEG-CIP-NLC formulations were comparatively higher than that with the CIP-NLCs. PEG(2K)-CIP-NLCs displayed higher entrapment efficiency – a 10% increase in entrapment in comparison to DSPE-CIP-NLCs. Zeta potential of DSPE-CIP-NLCs decreased with PEG derivatization from -12 to -2 mv, confirming surface charge neutralization by the PEG. Coating of the CIP-NLCs (DSPE-CIP-NLC) with chitosan (ChCl), on the other hand, increased the positive charge on the NLCs (Table 2).

3.2. Scanning transmission electron microscopy (STEM) studies

The STEM images of the representative samples are shown in Figure 1. STEM images of CIP NLCs showed the presence of spherical as well as rod-shaped nanoparticles whereas PEG-CIP-NLCs appeared to be spherical in shape with a well-defined periphery. Particle sizes obtained with TEM and DLS techniques may not be in agreement for the polydisperse formulations due to the respective operating principles and other contributing factors. Zeta sizer measures particle size based on intensity of scattered light whereas STEM measures it from each individual particle. Particle size agreements may hold true in monodisperse formulations (29–31).

3.3. Autoclave stability of CIP formulations

Physicochemical characteristics of the various NLC formulations, post terminal moist heat sterilization are presented in Table 3. Following sterilization, PEGylated NLCs were able to preserve their characteristics, whereas particle size and PDI was increased in the DSPE-CIP-NLCs and was also accompanied by a 14% decrease in entrapment efficiency. Moreover, the DSPE-CIP-NLC formulation was observed to be physically unstable (color, lipid phase separation) on steam sterilization. Addition of various reported stabilizing agents and cloud point modifiers such as polyvinyl pyrrolidone (PVP K30), polyvinyl alcohol (PVA Avg Mol wt 30K–70K Da), PEG 400, PEG 1000, PEG 4000, PEG 6000 at concentrations of 0.25% and 0.5% w/v in the DSPE-CIP-NLC formulations did not stabilize the phospholipids during the sterilization process.

Particle size and PDI of PEG-CIP-NLC formulations increased and entrapment efficiencies decreased as a function of increasing molecular weights of PEG (2K to 20K) used in the formulation. Moreover, PEG (20K)-CIP-NLCs appeared to be unstable during the sterilization process, with visible supernatant oil droplets. PEGs with molecular weights of up to 10K were observed to stabilize the DSPE-CIP-NLC formulations (Table 4).

Formulations (represented in tables 3 and 4) did not exhibit any statistically significant difference in physico-chemical characteristics, pre and post terminal moist heat sterilization except DSPE-CIP-NLCs and PEG(20K)-CIP-NLCs, which were unstable.

Studies were then undertaken to delineate the effect of the formulation components on autoclave stability. For this purpose, placebo formulations were used. Data on the effect of autoclaving on the physical stability of different placebo formulations, prepared using different lipids/phospholipids, is summarized in Table 5. Non-PEGylated NLCs prepared using phospholipids (DSPE) in combination with high melting triglyceride oils such as sesame, castor and soybean oils were stable post sterilization. NLCs prepared using a combination of the phospholipid with a fatty-acid (oleic acid) or caprylic/capric triglyceride (Miglyol®829) or Transcutol P were, however, unstable. These formulations were stabilized when PEGylated phospholipid (PEG(2K)-DSPE) was used - 50% of the total DSPE used was PEGylated in these experiments.

The effect of PEG concentration (surface packing density) on autoclave stability of phospholipid containing DSPE-CIP-NLC formulations is presented in Table 6. In these experiments the fraction of PEGylated lipid was varied from 0 to 40%, out of the total phospholipid content in the DSPE-CIP-NLCs, using PEG grafted lipids of different molecular weights - DSPE-PEG-1K/2K/5K. It was observed that DSPE-mPEG-5K stabilized the CIP-NLCs when used at a concentration of 30% w/w of total phospholipid in the formulation. Also, DSPE-mPEG-2K had to be used at a minimum of 40% w/w of the total phospholipid in the formulation for stabilization. Thus, higher molecular weight PEGs required lower PEGylated lipid concentrations to impart stability to the CIP-NLCs composition containing phospholipid and oleic acid.

3.4. *In vitro* release studies

These studies combined release and transmembrane diffusion – simulating ocular CIP penetration following topical application of the formulations. CIP flux from the DSPE-CIP-NLC and PEG(2K)-DSPE-CIP-NLC formulations, under the test conditions employed, were similar but the control formulation (0.3% Ophthalmic marketed control solution) showed a higher flux across the membrane – presumably because of the elimination of the release step from the process (Figure 2).

3.5. *In vitro* corneal permeation studies

In vitro transcorneal flux of CIP from the PEG(2K)-CIP-NLCs was almost 3-fold greater than that achieved with control solutions. CIP flux from the PEG(2K)-CIP-NLCs was about 2-fold higher compared to the DSPE-CIP-NLCs. Transcorneal flux of CIP from the chitosan coated NLCs (CIP-ChCl-NLC) was slightly better than that from the PEG(2K)-CIP-NLCs (Figure 3).

Carbon chain length of the phospholipid did not appear to affect transcorneal penetration of CIP from the PEG-CIP-NLCs. The molecular weight of PEG used to derivatize the phospholipid, however, had a significant effect on transcorneal flux of CIP (Figure 4). PEG (2K)-CIP-NLCs (DSPE-mPEG-2000) and PEG (5K)-CIP-NLCs (DSPE-mPEG-5000) enhanced transcorneal permeability of CIP by about 1.8-fold and 2.5-fold, respectively,

when compared to nonPEGylated CIP-NLCs (DSPE-CIP-NLCs). PEG (1K)-CIP-NLCs did not exhibit a significant increase over the CIP-NLCs. Thus, based on the data presented in Figures 3 and 4, it can be inferred that PEG-NLCs prepared with PEG-lipids with PEG molecular weights of 2K or greater are preferred to enhance ocular penetration of CIP.

In another set of studies, comparative corneal permeability of PEG-CIP-NLCs prepared with phospholipids (DSPE) grafted with higher molecular weight PEGs namely DSPE-PEG-2K/5K/10K/20K was determined. Although, transcorneal penetration of CIP exhibited an increasing trend with an increase in molecular weight of PEG from 2K to 10K, the difference in flux was not significantly different (Figure 5).

3.6. *In vivo* bioavailability studies

Following topical application of the formulations (Table 1) in conscious NZW rabbits, CIP levels in all ocular tissues tested, 2 h post dosing, were observed to be nearly 2-folds higher with the PEG(2K)-CIP-NLCs compared to DSPE-CIP-NLCs (non-PEGylated CIP-NLCs). The results were consistent with the *in vitro* observations. PEG(2K)-CIP-NLCs generated higher CIP concentrations in all ocular tissues tested except for the cornea – where CIP-ChCl-NLCs were observed to be slightly better (Figure 6).

Retinal CIP concentrations achieved with the PEG(2K)-CIP-NLCs is significantly higher compared to all other topical formulations. PEG(5K)-CIP-NLCs was similar, if not slightly better than the PEG(2K)-CIP-NLCs with respect to CIP levels obtained in the anterior segment tissues – AH, cornea and IC. CIP levels in the posterior segment or back-of-the eye tissues (retina-choroid) was, however, below detection levels with the PEG (5K)-CIP-NLCs. The PEG(10K)-CIP-NLCs and PEG(20K)-CIP-NLCs achieved much lower CIP concentrations in all ocular tissues tested in comparison to the PEG(2K)-CIP-NLCs (Figure 6). CIP concentrations in the AH and IC, achieved with the PEG(2K)-CIP-NLC and PEG(5K)-CIP-NLC formulations, were far greater than the minimum inhibitory concentration (MIC₉₀), approximately 0.5 µg/mL (32), even 2 h post topical dosing. In contrast, commercial CIP eye drops barely maintained MIC₉₀ levels in the AH, IC and cornea, 2 h post dosing, while CIP levels were undetectable or below MIC in the other ocular tissues tested.

4. Discussion

The focus of this project was to evaluate the effect of surface functionalization on ocular penetration of drugs from lipid nanocarriers and formulation stability. CIP was chosen as the model drug for preparing these formulations. Entrapment efficiency and release properties of drugs from lipid nanocarriers are highly dependent upon interfacial area, surface charge, inner structural organization, as well as nanoparticulate dimensions (33, 34). The size of the NPs plays a key role in their adhesion to and interaction with the biological cells. Smaller particles can be best internalized by receptor-mediate endocytosis uptake mechanism, while larger particles have to be taken up by phagocytosis (35–39).

In recent years, NLCs are increasingly being considered as viable carriers in drug delivery, but the present work introduces a new paradigm involving the concept of surface

functionalization/modification of nanoparticles and their sterilization - stabilization characteristics. Particle size and surface properties such as charge, morphology, hydrophilicity and surface modification with targeting ligand functionalization are the major controlling factors for interactions with the biological milieu (40, 41). Reports suggest that surface modification of nanoparticles by coating with hydrophilic substances such as PEGs could further improve ocular bioavailability, mainly due to enhanced interaction with ocular mucosal epithelium and decreased phagocytic uptake (42, 43). Fresta et al formulated PEG-6000 coated polyalkyl-2-cyanoacrylate nanosphere encapsulated acyclovir formulations and reported that the higher ocular bioavailability was achieved by polyalkyl-2-cyanoacrylate colloidal carrier, but no significant difference was observed between coated and uncoated nanospheres (44). These results may have resulted from a weak interaction of PEG molecules with the surface of colloidal particles. In the present project, we explored the effect of nanoparticle surface modification, by adsorption of Chitosan chloride or by firmly surface anchored PEG moieties, on ocular distribution and disposition. Also, the characteristics of the PEG's, optimal molecular weights and their relative concentrations needed to achieve improved penetration, was studied.

Drug release from the nanoparticles appears to be controlled by erosion and diffusion mechanisms through lipid matrix (45, 46). Interaction between nanoparticles and ocular epithelial cells could be attributed to endocytosis mechanism. Based on the transcorneal permeation data obtained, it could be said that penetration of CIP depends upon the molecular weight of grafted PEG's rather than it's carbon chain length (47). The permeability was not improved with PEG-1K and a decrease in the transmembrane flux was observed with PEG-20K, indicating the required range of molecular weights is between 2–10K for optimal penetration characteristics. The *in vitro* transcorneal permeability, an experimental set-up wherein the mucus layer is absent, data suggests that the PEGylation not only affects penetration across the mucus layer but also influences penetration across the corneal epithelial layers. When the PEG molecular weight went above 10K the penetration enhancing effect was lost, which could probably be because of the increased hydrophilicity and steric interference of the molecules. PEGylation range within which the formulations exert the optimal penetration and steric stabilization characteristics was further confirmed by the *in vivo* ocular distribution of CIP from the PEG-CIP-NLCs (Figure 6). PEGylated NLCs were able to deliver CIP, but penetration of CIP into posterior and anterior ocular tissues decreased as a function of increasing molecular weight of the PEG's (48, 49). These results indicate that the lipid conjugated PEGs with relatively higher molecular weights (greater than 5K) impart higher surface hydrophilicity onto the nanoparticles, which limits the penetration and partition of drugs across the surface mucus layer and epithelial membrane. The results were consistent with the *in vitro* observations. PEG-CIP-NLCs generated higher CIP concentrations in all ocular tissues except for the cornea – in which case ChCl-NLCs were observed to be slightly better (Figure 6). This, suggests that surface modification with chitosan favors retention of the nanoparticles at the superficial ocular layers (charge-charge interaction), whereas PEG grafting facilitates transport of the molecules across the mucus layers as well as the cornea and other ocular tissue, consistent with earlier reports (42, 50, 51).

Tai-Lee et al prepared two sustained release formulations of CIP using marketed CIP solution (0.3% w/v) with Dodecyl Maltoside as a penetration enhancer and carbopol/HPMC as viscosity enhancers. Two hours post-topical instillation (30 μ L), AH and corneal CIP concentrations obtained with HPMC and carbopol formulation were 0.5 μ g/mL and 4.2 μ g/g, respectively (52). Taha et al prepared ciprofloxacin loaded liposomes (0.3% w/v) and evaluated AH concentration after 2 h following topical application (50 μ L) in conscious rabbit model. The AH level was increased by \sim 0.3-fold when compared to marketed ophthalmic solution (53). In another study, 50 μ L of CIP loaded pluronic micelles (0.3 % w/v) enhanced AH concentration of CIP by 10%, 2 h post topical application, when compared to commercial CIP eye drops (54). In the present study ocular bioavailability of CIP was enhanced in the anterior and posterior segment ocular tissues, ranging from \sim 3–5-fold increase with PEG-CIP-NLC formulation, in comparison to control marketed formulation. This is significantly better than all earlier reports as well as the currently marketed ophthalmic formulation.

All ophthalmic products need to be sterilized. Autoclavable products are preferred, from a manufacturability point of view, over products that need aseptic processing or sterilization by filtration. Reports suggest that phospholipids undergo acidic/basic hydrolysis (pH < 5; pH > 9) and hence should be aseptically processed (55, 56). Our studies here demonstrate that selection of NLC formulation components can have a significant impact on the formulation stability during the sterilization process. Whereas long chain triglycerides components were stable, shorter chain length fatty acids and triglyceride containing NLCs could not withstand the autoclaving step. When a fraction of the phospholipids, in the heat unstable NLCs, were replaced with PEGylated phospholipids, the formulations are stabilized, suggesting that PEGs are able to preserve the supramolecular and molecular structure of colloids and protect the lipid environment. Addition of PEG externally or other known stabilizers to the NLCs did not impart thermal stability during the autoclave cycle. Additionally, it was observed that PEG-CIP-NLCs with PEG molecular weights of up to 10K stabilize the NLCs during the sterilization process, whereas PEG 20K fails to do so. Steric stabilization of liposomal formulations using PEG conjugated lipids is well documented in the literature (57–59). PEG has also been reported to be a surface modifying agent for improving permeability characteristics and decreasing phagocytic uptake of particulate drug carriers (60, 61). To the best of our knowledge, however, this is the first report that establishes the importance of the molecular weight and surface density of the PEG for preparing autoclave stable NLCs with enhanced transepithelial penetration and delivery characteristics, especially to the back-of-the eye tissues.

Interestingly, whereas chitosan chloride coated NLCs produced higher CIP concentrations in the cornea and sclera, the outer tunic of the eye, this did not translate into higher CIP penetration into the inner ocular layers. This, along with the observation that the CIP-NLCs (no surface modification) produced low CIP levels in all ocular tissues, suggests that PEGylation within the specified ranges improve transepithelial penetration of the CIP-NLCs into the deeper ocular tissues.

5. Conclusion

Surface functionalized nanostructured lipid carriers appear to be a promising and effective platform for topical ocular delivery. Surface modification strategies could improve ocular retention and intraocular penetration of therapeutics agents; thus enhancing ocular bioavailability and distribution. In conclusion, PEG grafted phospholipids/amphiphilic diblock copolymers with molecular weights in the range of 2K – 5K lead to optimal ocular penetration of molecules, including back-of-the eye and also autoclave stability.

Acknowledgments

This project was supported by grants 1R01EY022120-01A1 from the National Eye Institute and P20GM104932 from the National Institute of General Medical Sciences, National Institutes of Health. The content is solely the responsibility of the authors and does not necessarily represent the official views of the National Institutes of Health.

References

1. Gaudana R, Ananthula HK, Parenky A, Mitra AK. Ocular drug delivery. *AAPS J.* 2010; 12(3):348–60. [PubMed: 20437123]
2. Adelli GR, Balguri SP, Majumdar S. Effect of Cyclodextrins on Morphology and Barrier Characteristics of Isolated Rabbit Corneas. *AAPS PharmSciTech.* 2015; 16(5):1220–6. [PubMed: 25771740]
3. Cholkar K, Patel SP, Vadlapudi AD, Mitra AK. Novel strategies for anterior segment ocular drug delivery. *J Ocul Pharmacol Ther.* 2013; 29(2):106–23. [PubMed: 23215539]
4. Chen P, Chen H, Zang X, Chen M, Jiang H, Han S, et al. Expression of efflux transporters in human ocular tissues. *Drug Metab Dispos.* 2013; 41(11):1934–48. [PubMed: 23979916]
5. Patel A, Cholkar K, Agrahari V, Mitra AK. Ocular drug delivery systems: An overview. *World J Pharmacol.* 2013; 2(2):47–64. [PubMed: 25590022]
6. Yellepeddi VK, Palakurthi S. Recent Advances in Topical Ocular Drug Delivery. *J Ocul Pharmacol Ther.* 2016; 32(2):67–82. [PubMed: 26666398]
7. Geroski DH, Edelhauser HF. Drug Delivery for Posterior Segment Eye Disease. *Invest Ophthalmol Vis Sci.* 2000; 41(5):961–4. [PubMed: 10752928]
8. Adelli GR, Balguri SP, Bhagav P, Raman V, Majumdar S. Diclofenac sodium ion exchange resin complex loaded melt cast films for sustained release ocular delivery. *Drug Deliv.* 2017; 24(1):370–9. [PubMed: 28165833]
9. Sharma PKSP, Jaswanth A, Chalamaiiah M, Tekade KR, Balasubramaniam A. Novel Encapsulation of Lycopene in Niosomes and Assessment of its Anticancer Activity. *Journal of Bioequivalence & Bioavailability.* 2016; 8(5):224–32.
10. Singh VK, Singh PK, Sharma PK, Srivastava PK, Mishra A. Formulation and evaluation of topical gel of aceclofenac containing piparine. *Indo-American Journal of Pharmaceutical Research.* 2013; 3(7):5268.
11. Rowe-Rendleman CL, Durazo SA, Kompella UB, Rittenhouse KD, Di Polo A, Weiner AL, et al. Drug and gene delivery to the back of the eye: from bench to bedside. *Invest Ophthalmol Vis Sci.* 2014; 55(4):2714–30. [PubMed: 24777644]
12. Barar J, Aghanejad A, Fathi M, Omid Y. Advanced drug delivery and targeting technologies for the ocular diseases. *Bioimpacts.* 2016; 6(1):49–67. [PubMed: 27340624]
13. Adelli GR, Balguri SP, Punyamurthula N, Bhagav P, Majumdar S. Development and evaluation of prolonged release topical indomethacin formulations for ocular inflammation. *Invest Ophthalmol Vis Sci.* 2014; 55(13):463.
14. Maeda H, Bharate GY, Daruwalla J. Polymeric drugs for efficient tumor-targeted drug delivery based on EPR-effect. *Eur J Pharm Biopharm.* 2009; 71(3):409–19. [PubMed: 19070661]

15. Barenholz Y. Doxil® — The first FDA-approved nano-drug: Lessons learned. *J Control Release*. 2012; 160(2):117–34. [PubMed: 22484195]
16. Kompella UB, Amrite AC, Pacha Ravi R, Durazo SA. Nanomedicines for back of the eye drug delivery, gene delivery, and imaging. *Prog Retin Eye Res*. 2013; 36:172–98. [PubMed: 23603534]
17. Yoon G, Park JW, Yoon I-S. Solid lipid nanoparticles (SLNs) and nanostructured lipid carriers (NLCs): recent advances in drug delivery. *Journal of Pharmaceutical Investigation*. 2013; 43(5): 353–62.
18. Müller RH, Radtke M, Wissing SA. Solid lipid nanoparticles (SLN) and nanostructured lipid carriers (NLC) cosmetic and dermatological preparations. *Adv Drug Deliv Rev*. 2002; 54(Supplement):S131–S55. [PubMed: 12460720]
19. Tiwari R, Pathak K. Nanostructured lipid carrier versus solid lipid nanoparticles of simvastatin: comparative analysis of characteristics, pharmacokinetics and tissue uptake. *Int J Pharm*. 2011; 415(1–2):232–43. [PubMed: 21640809]
20. Chen Y, Ma P, Gui S. Cubic and hexagonal liquid crystals as drug delivery systems. *Biomed Res Int*. 2014; 2014:815981. [PubMed: 24995330]
21. Balguri SP, Adelli G, Bhagav P, Repka MA, Majumdar S. Development of nano structured lipid carriers of ciprofloxacin for ocular delivery: Characterization, in vivo distribution and effect of PEGylation. *Invest Ophthalmol Vis Sci*. 2015; 56(7):2269. [PubMed: 25744979]
22. Zheng J, Wan Y, Elhissi A, Zhang Z, Sun X. Targeted paclitaxel delivery to tumors using cleavable PEG-conjugated solid lipid nanoparticles. *Pharm Res*. 2014; 31(8):2220–33. [PubMed: 24595496]
23. Schilt Y, Berman T, Wei X, Barenholz Y, Raviv U. Using solution X-ray scattering to determine the high-resolution structure and morphology of PEGylated liposomal doxorubicin nanodrugs. *Biochim Biophys Acta*. 2016; 1860(1 Pt A):108–19. [PubMed: 26391840]
24. Kakkar S, Karuppaiyl SM, Raut JS, Giansanti F, Papucci L, Schiavone N, et al. Lipid-polyethylene glycol based nano-ocular formulation of ketoconazole. *Int J Pharm*. 2015; 495(1):276–89. [PubMed: 26325312]
25. Balguri SP, Adelli GR, Majumdar S. Topical ophthalmic lipid nanoparticle formulations (SLN, NLC) of indomethacin for delivery to the posterior segment ocular tissues. *Eur J Pharm Biopharm*. 2016; 109:224–35. [PubMed: 27793755]
26. Hosny KM. Ciprofloxacin as ocular liposomal hydrogel. *AAPS PharmSciTech*. 2010; 11(1):241–6. [PubMed: 20151337]
27. Hussain AH, Muhammad Shoaib, Muhammad Harris, Yousuf, Rabia Ismail, Shafi Nigha. Bioanalytical method development and validation of ciprofloxacin by RP-HPLC method. *Asian Journal of Pharmaceutical & Biological Research* October. 2012; 2(4):219.
28. Guidance for Industry: Bioanalytical Method Validation. 2013. [Available from: <https://www.fda.gov/downloads/Drugs/Guidances/ucm368107.pdf>]
29. Lizunova A, Loshkarev A, Tokunov YM, Ivanov V. Comparison of the Results of Measurements of the Sizes of Nanoparticles in Stable Colloidal Solutions by the Methods of Acoustic Spectroscopy, Dynamic Light Scattering, and Transmission Electron Microscopy. *Measurement Techniques*. 2017:1–5.
30. Anderson W, Kozak D, Coleman VA, Jämting ÅK, Trau M. A comparative study of submicron particle sizing platforms: accuracy, precision and resolution analysis of polydisperse particle size distributions. *Journal of colloid and interface science*. 2013; 405:322–30. [PubMed: 23759321]
31. Tuoriniemi J, Johnsson A-CJ, Holmberg JP, Gustafsson S, Gallego-Urrea JA, Olsson E, et al. Intermethod comparison of the particle size distributions of colloidal silica nanoparticles. *Science and Technology of Advanced Materials*. 2014; 15(3):035009. [PubMed: 27877685]
32. Morlet N, Graham GG, Gatus B, McLachlan AJ, Salonikas C, Naidoo D, et al. Pharmacokinetics of ciprofloxacin in the human eye: a clinical study and population pharmacokinetic analysis. *Antimicrobial agents and chemotherapy*. 2000; 44(6):1674–9. [PubMed: 10817727]
33. Lim SB, Banerjee A, Onyuksel H. Improvement of drug safety by the use of lipid-based nanocarriers. *J Control Release*. 2012; 163(1):34–45. [PubMed: 22698939]
34. Martins S, Sarmiento B, Ferreira DC, Souto EB. Lipid-based colloidal carriers for peptide and protein delivery—liposomes versus lipid nanoparticles. *Int J Nanomedicine*. 2007; 2(4):595–607. [PubMed: 18203427]

35. Kulkarni SA, Feng SS. Effects of particle size and surface modification on cellular uptake and biodistribution of polymeric nanoparticles for drug delivery. *Pharm Res.* 2013; 30(10):2512–22. [PubMed: 23314933]
36. He C, Hu Y, Yin L, Tang C, Yin C. Effects of particle size and surface charge on cellular uptake and biodistribution of polymeric nanoparticles. *Biomaterials.* 2010; 31(13):3657–66. [PubMed: 20138662]
37. Kou L, Sun J, Zhai Y, He Z. The endocytosis and intracellular fate of nanomedicines: Implication for rational design. *Asian Journal of Pharmaceutical Sciences.* 2013; 8(1):1–10.
38. Qaddoumi MG, Ueda H, Yang J, Davda J, Labhasetwar V, Lee VHL. The Characteristics and Mechanisms of Uptake of PLGA Nanoparticles in Rabbit Conjunctival Epithelial Cell Layers. *Pharm Res.* 2004; 21(4):641–8. [PubMed: 15139521]
39. Contreras-Ruiz L, de la Fuente M, Parraga JE, Lopez-Garcia A, Fernandez I, Seijo B, et al. Intracellular trafficking of hyaluronic acid-chitosan oligomer-based nanoparticles in cultured human ocular surface cells. *Mol Vis.* 2011; 17:279–90. [PubMed: 21283563]
40. Tosi G, Vergoni AV, Ruozi B, Bondioli L, Badiali L, Rivasi F, et al. Sialic acid and glycopeptides conjugated PLGA nanoparticles for central nervous system targeting: In vivo pharmacological evidence and biodistribution. *J Control Release.* 2010; 145(1):49–57. [PubMed: 20338201]
41. Vergoni AV, Tosi G, Tacchi R, Vandelli MA, Bertolini A, Costantino L. Nanoparticles as drug delivery agents specific for CNS: in vivo biodistribution. *Nanomedicine.* 2009; 5(4):369–77. [PubMed: 19341816]
42. De Campos AM, Sánchez A, Gref R, Calvo P, Alonso M, et al. The effect of a PEG versus a chitosan coating on the interaction of drug colloidal carriers with the ocular mucosa. *Eur J Pharm Sci.* 2003; 20(1):73–81. [PubMed: 13678795]
43. Giannavola C, Bucolo C, Maltese A, Paolino D, Vandelli MA, Puglisi G, et al. Influence of Preparation Conditions on Acyclovir-Loaded Poly-D,L-Lactic Acid Nanospheres and Effect of PEG Coating on Ocular Drug Bioavailability. *Pharm Res.* 2003; 20(4):584–90. [PubMed: 12739765]
44. Fresta M, Fontana G, Bucolo C, Cavallaro G, Giammona G, Puglisi G. Ocular tolerability and in vivo bioavailability of poly(ethylene glycol) (PEG)-coated polyethyl-2-cyanoacrylate nanosphere-encapsulated acyclovir. *J Pharm Sci.* 2001; 90(3):288–97. [PubMed: 11170022]
45. Zeng N, Hu Q, Liu Z, Gao X, Hu R, Song Q, et al. Preparation and characterization of paclitaxel-loaded DSPE-PEG-liquid crystalline nanoparticles (LCNPs) for improved bioavailability. *Int J Pharm.* 2012; 424(1–2):58–66. [PubMed: 22240390]
46. Adelli GR, Hingorani T, Punyamurthula N, Balguri SP, Majumdar S. Evaluation of topical hesperetin matrix film for back-of-the-eye delivery. *Eur J Pharm Biopharm.* 2015; 92:74–82. [PubMed: 25728824]
47. Pozzi D, Colapicchioni V, Caracciolo G, Piovesana S, Capriotti AL, Palchetti S, et al. Effect of polyethyleneglycol (PEG) chain length on the bio-nano-interactions between PEGylated lipid nanoparticles and biological fluids: from nanostructure to uptake in cancer cells. *Nanoscale.* 2014; 6(5):2782–92. [PubMed: 24463404]
48. Veronese FM, Pasut G. PEGylation, successful approach to drug delivery. *Drug Discov Today.* 2005; 10(21):1451–8. [PubMed: 16243265]
49. Veronese FM, Mero A. The impact of PEGylation on biological therapies. *BioDrugs.* 2008; 22(5): 315–29. [PubMed: 18778113]
50. Vij N, Min T, Marasigan R, Belcher CN, Mazur S, Ding H, et al. Development of PEGylated PLGA nanoparticle for controlled and sustained drug delivery in cystic fibrosis. *J Nanobiotechnology.* 2010; 8(1):22. [PubMed: 20868490]
51. Li W, Zhan P, De Clercq E, Lou H, Liu X. Current drug research on PEGylation with small molecular agents. *Prog Polym Sci.* 2013; 38(3–4):421–44.
52. Ke TL, Cagle G, Schleich B, Lorenzetti OJ, Mattern J. Ocular bioavailability of ciprofloxacin in sustained release formulations. *J Ocul Pharmacol Ther.* 2001; 17(6):555–63. [PubMed: 11777179]
53. Taha EI, El-Anazi MH, El-Bagory IM, Bayomi MA. Design of liposomal colloidal systems for ocular delivery of ciprofloxacin. *Saudi Pharmaceutical Journal.* 2014; 22(3):231–9. [PubMed: 25061409]

54. Taha EI, Badran MM, El-Anazi MH, Bayomi MA, El-Bagory IM. Role of Pluronic F127 micelles in enhancing ocular delivery of ciprofloxacin. *J Mol Liq.* 2014; 199:251–6.
55. Hui PK, Diluzio WR. Stabilization and terminal sterilization of phospholipid formulations. Google Patents. 2002
56. Mishra AK. Thermoprotected compositions and process for terminal steam sterilization of microparticle preparations. Google Patents. 2013
57. Allen TM, Hansen C, Martin F, Redemann C, Yau-Young A. Liposomes containing synthetic lipid derivatives of poly(ethylene glycol) show prolonged circulation half-lives in vivo. *Biochim Biophys Acta.* 1991; 1066(1):29–36. [PubMed: 2065067]
58. Woodle MC, Newman MS, Cohen JA. Sterically stabilized liposomes: physical and biological properties. *J Drug Target.* 1994; 2(5):397–403. [PubMed: 7704484]
59. Woodle MC. Sterically stabilized liposome therapeutics. *Advanced Drug Delivery Reviews.* 1995; 16(2):249–65.
60. Uner M, Yener G. Importance of solid lipid nanoparticles (SLN) in various administration routes and future perspectives. *Int J Nanomedicine.* 2007; 2(3):289–300. [PubMed: 18019829]
61. Verhoef JJF, Anchordoquy TJ. Questioning the use of PEGylation for drug delivery. *Drug Deliv Transl Res.* 2013; 3(6):499–503. [PubMed: 24932437]

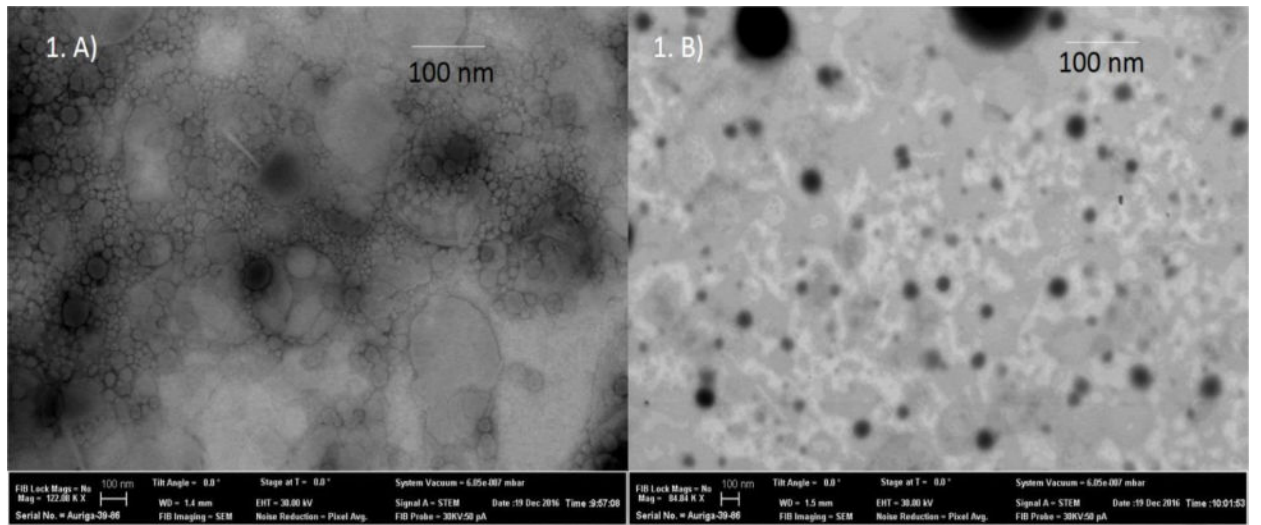


Figure 1.
STEM images of CIP loaded NLCs. A) CIP NLCs. B) PEG(2K)-CIP-NLCs.

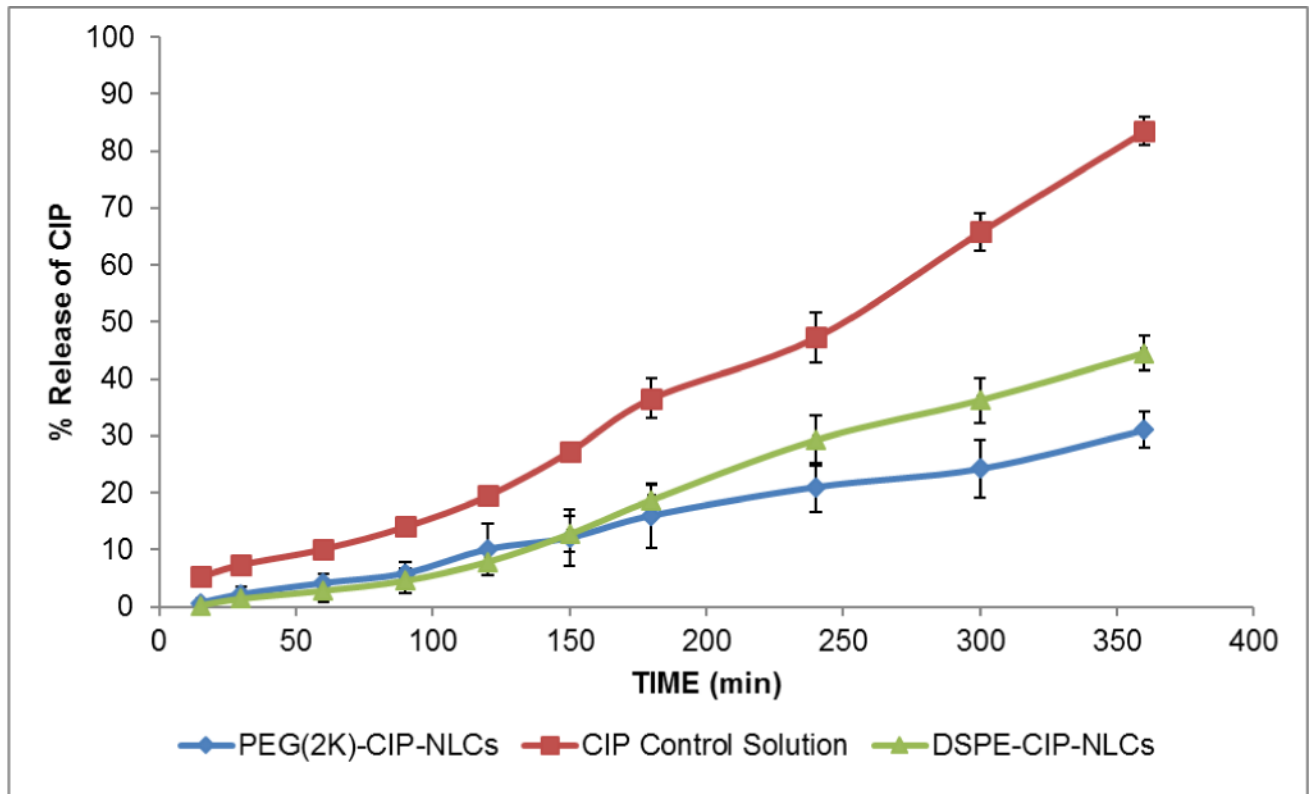


Figure 2.

In vitro release of CIP obtained across Spectra/Por[®] membrane (MWCO: 3.5 KDa) from CIP loaded PEGylated NLCs (PEG(2K)-CIP-NLCs), 0.3% w/v CIP ophthalmic Solution, and CIP-NLCs (DSPE-CIP-NLCs) obtained using Valia-Chien cells at 34°C. (Dose: 500 μ L; 1500 μ g).

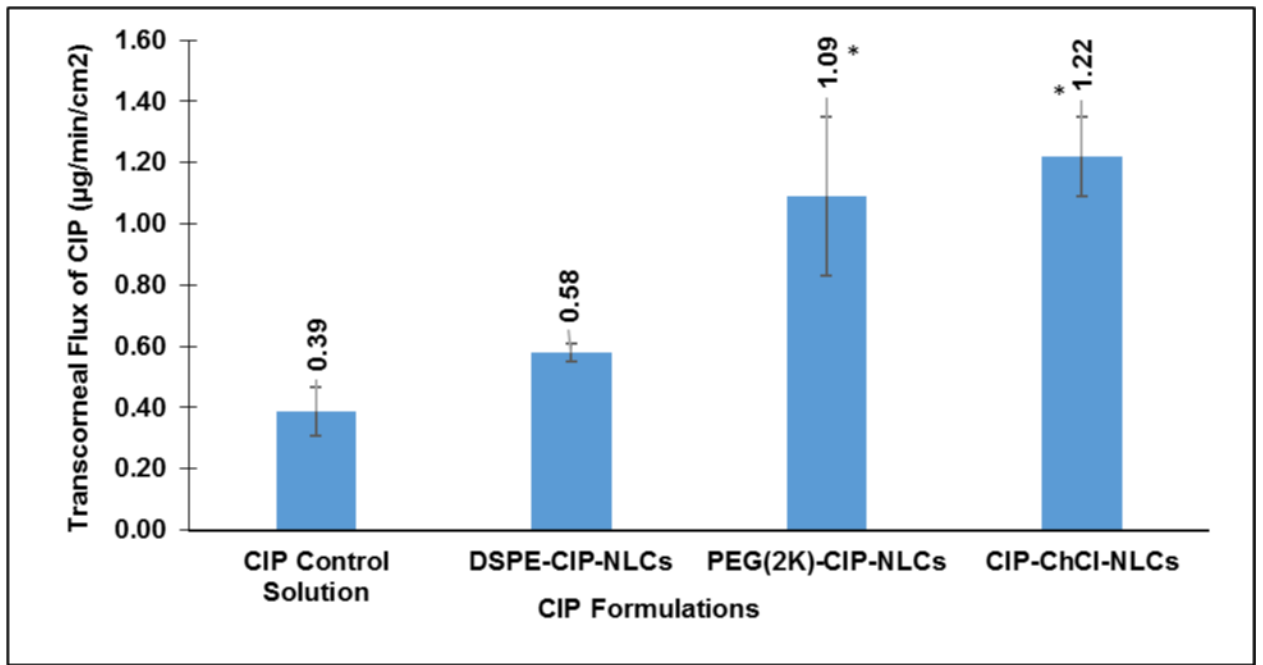


Figure 3.

Transcorneal flux of CIP obtained from CIP ophthalmic Solution, DSPE-CIP-NLCs, PEG(2K)-CIP-NLCs and Chitosan Chloride coated DSPE-CIP-NLCs (CIP-ChCl-NLCs) using Valia-Chien cells at 34°C (Dose: 500 µL; 1500 µg; n=4). * symbol denotes statistical significance of PEG(2K)-CIP-NLCs and CIP-ChCl-NLCs when compared to control and DSPE-CIP-NLCs ($p < 0.05$).

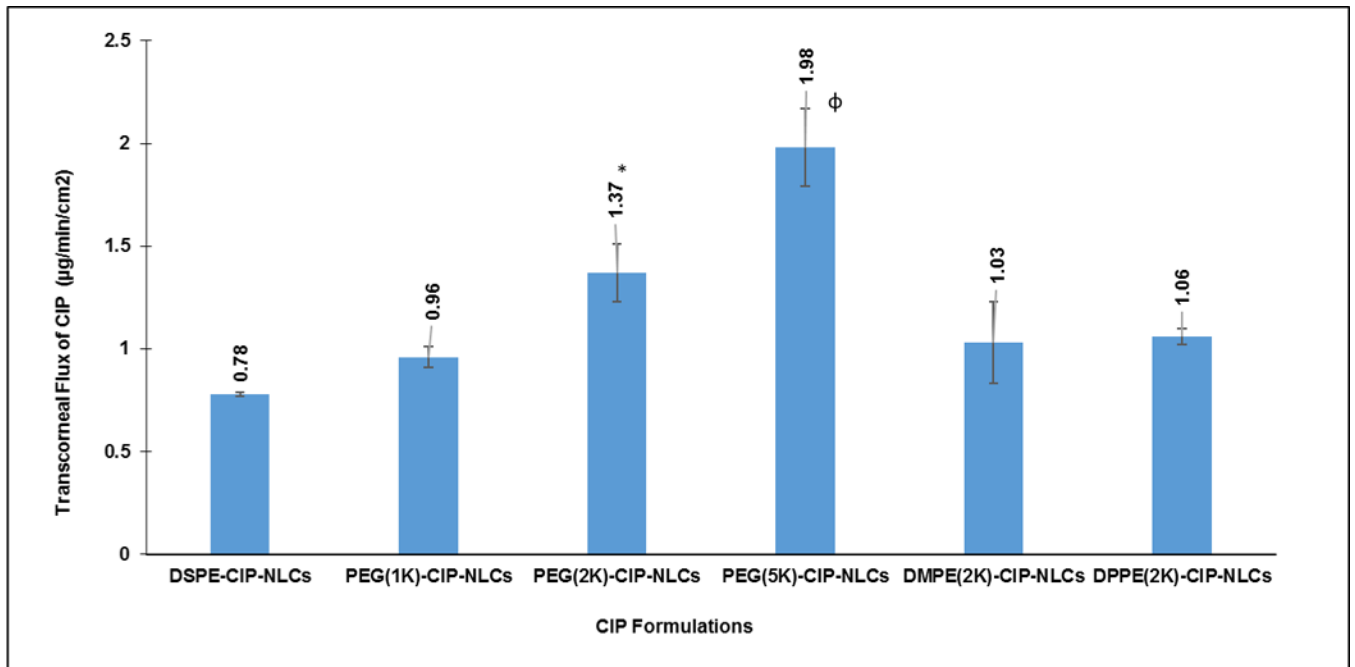


Figure 4.

Transcorneal flux of CIP obtained from various topical NLC formulations tested with different molecular weights of PEG grafted, DSPE phospholipid (PEG-1K (PEG(1K)-CIP-NLCs/2K (PEG(2K)-CIP-NLCs/5K (PEG(5K)-CIP-NLCs) and varied chain lengths of PEG-2000 conjugated phospholipids (DMPE(2K)-CIP-NLCs, DPPE(DPPE(2K)-CIP-NLCs) using side-by-side diffusion cells (PermeGear, Inc) at 34°C (Dose: 3 mL; 0.3% w/v) (n=4). * symbol denotes statistically significant difference of CIP flux from PEG(2K)-CIP-NLCs when compared to DSPE-CIP-NLCs whereas ϕ symbol indicates statistically significant difference of CIP flux from PEG(5K)-CIP-NLCs in comparison to all the formulations ($p < 0.05$).

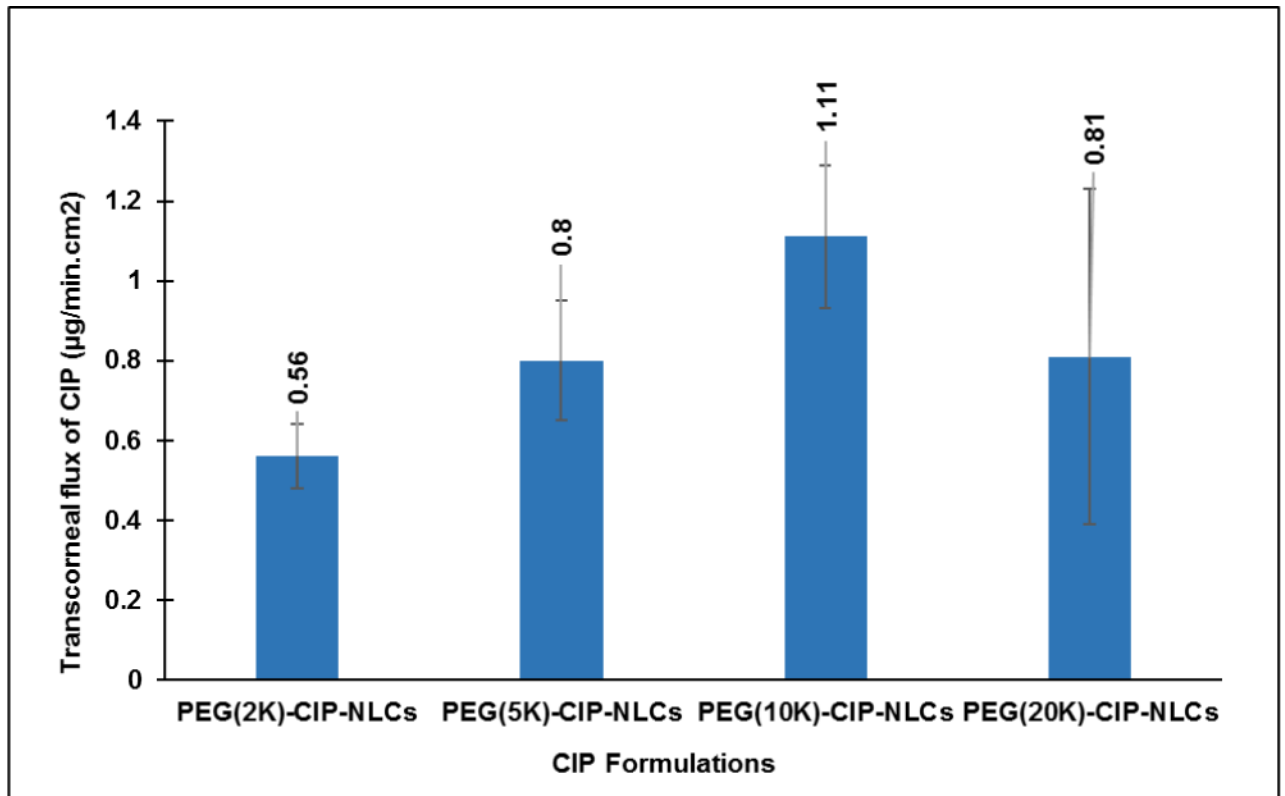


Figure 5. Transcorneal flux of CIP obtained from NLC systems with higher molecular weights of PEG's grafted to DSPE phospholipid (2K/5K/10K (PEG (10K)-CIP-NLCs/20K (PEG (20K)-CIP-NLCs), using side-by-side cells at 34° C (Dose: 3 mL; 0.3% w/v; n=4).

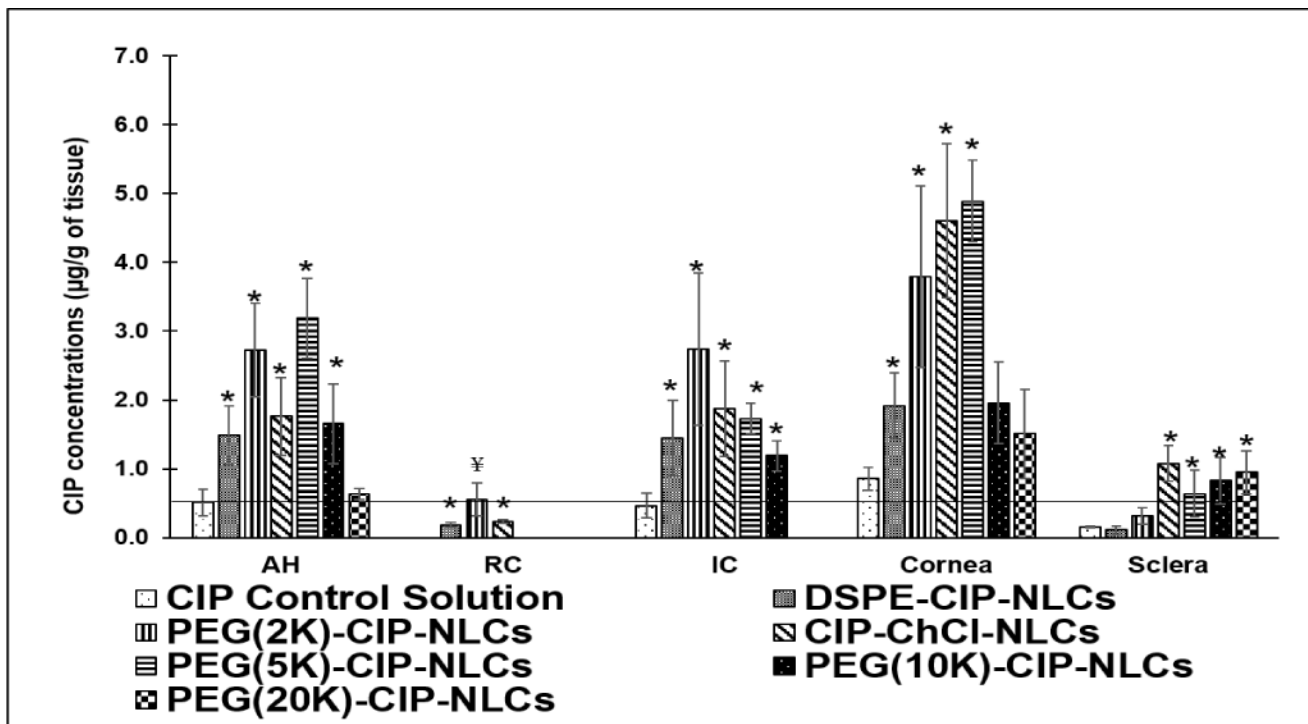


Figure 6.

Ocular tissue concentrations of CIP obtained from CIP Ophthalmic control Solution, DSPE-CIP-NLCs, Chitosan coated DSPE-CIP-NLCs (CIP-ChCl-NLCs) and CIP loaded PEGylated NLCs with different molecular weights of PEGs (DSPE-PEG-2K, DSPE-PEG-5K, DSPE-10K, DSPE-20K) 2 h post topical application (Dose: 300 µg; 100 µL at -30 and 0 min) in a conscious rabbit model. (AH-Aqueous humor, IC-Iris ciliary bodies and RC-Retina choroid). MIC90 of CIP is marked as a horizontal line in the figure. Statistical analysis by One way ANOVA with post-hoc test was performed, where symbol (*) on the ocular tissues represent statistically significant difference of CIP concentrations from different formulations in comparison to control solution. (¥) represents statistically significant difference of retinal concentrations obtained from PEG (2K)-CIP-NLCs compared to all the formulations.

Composition of CIP-NLCs and PEGylated CIP-NLCs (PEG-CIP-NLC) formulations. Various PEG-CIP-NLCs were prepared using PEG conjugated phospholipids of different carbon chain lengths and PEG molecular weights.

Table 1

Formulations	CIP (mg)	Oleic acid (liquid lipid - mg)	GMS (solid lipid -mg)	Phospholipid (mg)	PEGylated Phospholipid (mg)	Chitosan Chloride	Poloxamer 188 (mg)	Tween® 80 (mg)	Glycerin (mg)	Water (mL)
CIP-NLCs										
DMPE-CIP-NLCs	30	300	150	150 (DMPE)	-	-	25	75	225	10
DPPE-CIP-NLCs	30	300	150	150 (DPPE)	-	-	25	75	225	10
DSPE-CIP-NLCs	30	300	150	150 (DSPE)	-	-	25	75	225	10
PEGylated CIP-NLCs (PEG-CIP-NLCs)										
PEG(1K)-CIP-NLCs	30	300	150	-	150 (DSPE-PEG-1K)	-	25	75	225	10
PEG(2K)-CIP-NLCs	30	300	150	-	150 (DSPE-PEG-2K)	-	25	75	225	10
PEG(5K)-CIP-NLCs	30	300	150	-	150 (DSPE-PEG-5K)	-	25	75	225	10
PEG(10K)-CIP-NLCs	30	300	150	-	150 (DSPE-PEG-10K)	-	25	75	225	10
PEG(20K)-CIP-NLCs	30	300	150	-	150 (DSPE-PEG-20K)	-	25	75	225	10
DMPE(2K)-CIP-NLCs	30	300	150	-	150 (DMPE-PEG-2K)	-	25	75	225	10
DPPE(2K)-CIP-NLCs	30	300	150	-	150 (DPPE-PEG-2K)	-	25	75	225	10
Chitosan coated CIP-NLCs (CIP-ChCl-NLCs)										
CIP-ChCl-NLCs	30	300	150	150 (DSPE)	-	25	25	75	225	10

Table 2
Physicochemical characteristics of CIP-NLCs and PEGylated CIP-NLC formulations

Characteristics	PEGylated CIP-NLCs						Chitosan coated CIP-NLCs	
	CIP-NLCs	PEG(1K)-IP-NLCs	PEG(2K)-CIP-NLCs	PEG(5K)-CIP-NLCs	DMPE(2K)-CIP-NLCs	DPPE(2K)-CIP-NLCs	CIP-ChCl-NLCs	
Particle size (nm)	190±15	165±12	180.6±13	217±18	176±4.8	184±3.6	220±16	
Polydispersity index (PDI)	0.26±0.03	0.29±0.01	0.31±0.01	0.37±0.03	0.28±0.02	0.27±0.03	0.33±0.06	
Zeta potential (mV)	-12.2±1.08	-1.0±0.02	-1.8±0.08	-2.6±0.06	-2.3±0.03	-2.1±0.06	29.2±3.9	
Entrapment Efficiency (% EE)	72.5±3.9	79.6±2.4	83.6±4.7	84.2±2.3	79.8±1.9	81.2±2	73.6±3.6	
Assay (%)	CIP content was 90–95% of the theoretical value in all the formulations							

Table 3
Effect of autoclaving on the physicochemical attributes of CIP-NLCs and PEG-CIP-NLCs (pre and post sterilization).

Formulations	Particle Size (nm)		Polydispersity index (PDI)		Assay		pH		Zeta potential (mV)	
	Sterilization Stage		Sterilization Stage		Sterilization Stage		Sterilization Stage		Sterilization Stage	
	Pre	Post	Pre	Post	Pre	Post	Pre	Post	Pre	Post
DSPE-CIP-NLCs	190±15	230±7.5	0.26±0.03	0.35±0.05	90.9±4.5	87.1±2.1	5	3.6	-12.2±1.08	-14.6±1.95
PEG(1K)-CIP-NLCs	165±12	169±8	0.29±0.01	0.29±0.02	90.2±2.8	89.1±2.6	5	4.76	-1.0±0.02	-1.12±0.01
PEG(2K)-CIP-NLCs	180.6±13	192±8	0.31±0.01	0.32±0.01	90.1±3.1	88.4±3.6	5	4.8	-1.8±0.08	-1.9±0.06
PEG(5K)-CIP-NLCs	217±18	231±9.1	0.37±0.03	0.42±0.02	92.6±1.8	91.9±2.9	5	4.4	-2.6±0.06	-3.4±0.04
DMPE(2K)-CIP-NLCs	176±4.8	191±7.6	0.28±0.02	0.31±0.04	91.4±1.1	89.4±0.67	5	4.58	-2.3±0.03	-2.9±0.053
DPPE(2K)-CIP-NLCs	184±3.6	189±8.5	0.27±0.03	0.3±0.02	93.2±0.9	91.8±1.2	5	4.82	-2.1±0.06	-3.3±0.04

Effect of autoclaving on the physicochemical characteristics of PEG-CIP-NLC formulations prepared with higher molecular weight PEG's pre and post sterilization.

Table 4

Formulations (PEGylated CIP-NLCs)	Particle Size (nm)		Polydispersity Index (PDI)		Entrapment efficiency (%EE)		Zeta potential (mV)	
	Sterilization Stage		Sterilization Stage		Sterilization Stage		Sterilization Stage	
	Pre	Post	Pre	Post	Pre	Post	Pre	Post
PEG(2K)-CIP-NLCs	175.6±13	172±8	0.27±0.02	0.26±0.03	88.8±2.2	88.1±0.7	-0.4±0.03	-0.7±0.06
PEG(5K)-CIP-NLCs	207±9	209±12	0.31±0.02	0.32±0.04	80.4±6.7	76.9±2.3	-1.9±0.06	-2.1±0.03
PEG(10K)-CIP-NLCs	280±7	297±11.3	0.36±0.04	0.42±0.07	76.1±4.51	69.2±4.27	-1.4±0.07	-1.5±0.02
PEG(20K)-CIP-NLCs	320±18	cracked	0.45±0.07	cracked	73.6±9.68	cracked	-0.2±0.03	cracked

Table 5

Physical stability of placebo NLC formulations (n=2) prepared with different lipids (solid and/or liquid) post autoclave sterilization.

Formulation	Solid lipid (mg)	Liquid lipid (mg)	Poloxamer 188 (mg)	Tween®80 (mg)	Glycerin (mg)	Result
F-1	GMS (400)	-	5	-	-	No change
F-2	GMS, DSPE (1:1) 9 parts (270, 270)	Oleic acid 1 part (60) total 9:1 (S:L)	25	75	225	Failed
F-3	Precirol (360) 9 parts	Oleic acid 1 part (40) total 9:1 (S:L)	-	250	-	Discoloration in one formulation
F-4	GMS (300) 3 parts	Castor oil (100) 1 part ; 3:1 (S:L)	5	-	-	No change
F-5	Compritol (200)	Castor oil (200)	25	75	225	No change
F-6	GMS (200)	Castor oil (200)	25	75	225	No change
F-7	GMS (200)	Oleic acid (200)	25	75	225	No change
F-8	GMS (300)	Soyabean oil (300)	25	75	225	No change
F-9	GMS, DSPE (150,150) (1:1)	Soyabean oil (300)	25	75	225	No change
F-10	GMS (300)	Sesame oil (300)	25	75	225	No change
F-11	GMS, DSPE (150,150) (1:1)	Sesame oil (300)	25	75	225	No change
F-12	GMS, DSPE (150,150) (1:1)	Castor oil (300)	25	75	225	No change
F-13	GMS (300)	Miglyol 829 (300)	25	75	225	No change
F-14	GMS, DSPE (150,150) (1:1)	Miglyol 829 (300)	25	75	225	Discoloration
F-15	GMS (300)	Capryol 90 (300)	25	75	225	No change
F-16	GMS, DSPE (150,150) (1:1)	Capryol 90 (300)	25	75	225	No change
F-17	GMS (300)	Lauroglycol (300)	25	75	225	No change
F-18	GMS, DSPE (150,150) (1:1)	Lauroglycol (300)	25	75	225	No change
F-19	GMS (300)	Lauroglycol (300)	25	75	225	No change
F-20	GMS, DSPE (150,150) (1:1)	Lauroglycol (300)	25	75	225	No change
F-21	GMS (300)	Labrafac (300)	25	75	225	No change
F-22	GMS, DSPE (150,150) (1:1)	Labrafac (300)	25	75	225	No change
F-23	GMS (300)	Isopropyl Myristate (300)	25	75	225	No change
F-24	GMS, DSPE (150,150) (1:1)	Isopropyl Myristate (300)	25	75	225	No change
F-25	GMS (300)	Labrafil (300)	25	75	225	No change
F-26	GMS, DSPE (150,150) (1:1)	Labrafil (300)	25	75	225	No change
F-27	GMS (300)	Transcutol (300)	25	75	225	No change

Formulation	Solid lipid (mg)	Liquid lipid (mg)	Poloxamer 188 (mg)	Tween®80 (mg)	Glycerin (mg)	Result
F-28	GMS, DSPE (150,150) (1:1)	Transcutol (300)	25	75	225	Failed

Author Manuscript

Author Manuscript

Author Manuscript

Author Manuscript

Effect of PEGylated to unPEGylated phospholipid ratio and PEG molecular weight on physical stability of placebo PEG-NLC post autoclave sterilization.

Table 6

% of PEG-lipid	DSPE-PEG-1K/2K/5K lipid (mg)	DSPE lipid (mg)	Oleic acid (mg)	GMS (mg)	Result
PEG(1K)-CIP-NLCs					
15	22.5	127.5	300	150	Cracked
30	45	105	300	150	Cracked
40	60	90	300	150	Cracked
PEG(2K)-CIP-NLCs					
0 (Control)	(0)	150	300	150	Cracked
10	15	135	300	150	Cracked
15	22.5	127.5	300	150	Cracked
25	37.5	112.5	300	150	Cracked
30	45	105	300	150	Droplets
35	52.5	97.5	300	150	Droplets
40	60	90	300	150	No change
PEG(5K)-CIP-NLCs					
15	22.5	127.5	300	150	Cracked
30	45	105	300	150	No change